Modulation of Heterogeneous Electron-Transfer Dynamics Across the Electrode/Monolayer Interface

Darren A. Walsh, Tia E. Keyes, and Robert J. Forster*

National Center for Sensor Research, Dublin City University, Glasnevin, Dublin 9, Ireland

Received: August 29, 2003; In Final Form: December 9, 2003

Spontaneously adsorbed monolayers of $[Os(bpy)_2 4bptCl](PF_6)$ have been formed on platinum microelectrodes. bpy is 2,2′-bipyridyl, and 4bpt is 3,5-bis(pyridin-4-yl)-1,2,4-triazole. These monolayers exhibit well-defined, almost ideal electrochemical responses over a wide range of voltammetric scan rates and in a wide range of electrolytic solutions. The surface coverage of these monolayer films is consistent with that expected for a close-packed monolayer, in which the area of occupation is governed by the area of the redox-active headgroup rather than by the bridging ligand. The differential capacitance of the monolayer-modified interface is 18 ± 3 μF cm^{-2} compared to 35 ± 3 μF cm^{-2} for an unmodified surface. Consistent with the observation that the formal potential of the $Os^{2+/3+}$ process shifts by less than 30 mV upon immobilization, these data suggest that the monolayers are well solvated. The dependence of the differential capacitance on solution pH reveals that the pK_a of the triazole bridge within the monolayer, 8.9 ± 0.3, is indistinguishable from that found in solution. Chronoamperometry, conducted on a nanosecond time scale, reveals that the redox switching mechanism involves hole rather than electron transfer. Significantly, upon protonation of the 4bpt bridging ligand, the standard heterogeneous hole transfer rate constant decreases from 1.60 to 0.2×10^6 s^{-1} for the reduction mechanism and from 2.7 to 0.05×10^6 s^{-1} for the oxidation process. These observations are consistent with the redox mechanism occurring via a hole-transfer process, the rate of which depends on the energy difference between the metal d π orbitals and the HOMO of the bridge. Protonation of the bridging ligand increases this energy gap, resulting in an overall decrease in the rate of the redox reaction.

Introduction

Bridge-mediated electron- and hole-transfer reactions are crucially important to areas as diverse as understanding biological electron-transfer mechanisms, e.g., in photosynthesis,[1,2,3] to the development of "molecular wires" with applications in molecular electronics.[4,5] The roles of distance,[6,7] driving force,[8,9] and electrolyte[10,11,12,13] on the dynamics of electron transfer have been studied extensively to date. However, one important area that remains underexplored is how to reversibly and easily modulate the rate of electron transfer across molecular linkers. Significant advances in this area have been made by synthetically altering the structure of the intervening bridge between redox sites,[14,15,16,17] but this approach requires considerable synthetic skill and does not allow the energy difference between donor/acceptor and the bridge to be reversibly and arbitrarily varied.

When electron transfer occurs via a superexchange mechanism,[18] the difference in energy of the donor/acceptor and bridge states levels will influence the relative rates of electron transfer. If the energy difference between the donor/acceptor (D/A) orbitals and the HOMO of the bridge is smaller than the D/A-LUMO separation, then the redox mechanism is likely to occur via a hole-superexchange mechanism. Therefore, by tuning the position of the bridge HOMO or LUMO, it ought to be possible to modulate the rate of redox switching.

In this contribution, we report on monolayers in which $[Os(bpy)_2Cl]^+$ groups are tethered to platinum microelectrode surfaces via the bridging ligand 3,5-bis(pyridin-4-yl)-1,2,4-triazole (4bpt, Chart 1). Previous investigations suggested that the protonated form of this bridge supports hole superexchange.[19] The electrochemical responses of these monolayers are unusually ideal and, significantly, this bridging ligand is capable of undergoing a protonation/deprotonation reaction depending on the pH of the contacting electrolyte solution. The pH dependence of the interfacial capacitance has been used to determine the effect of immobilization of the triazole pK_a and the extent to which the monolayers are solvated. We have used high-speed chronoamperometry to probe the pH dependence of the redox switching rate. Deprotonation of the bridge causes

CHART 1

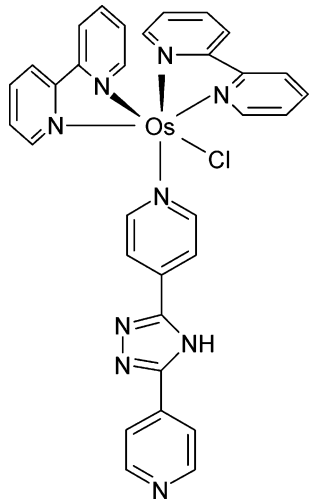

* Author to whom correspondence should be addressed. E-mail: robert.forster@dcu.ie.

10.1021/jp036577v CCC: $27.50
Published on Web 01/21/2004

an increase in the rate of heterogeneous electron dynamics by at least 1 order of magnitude. This is interpreted in terms of a change in the energy difference between the $Os_{d\tau}$ orbitals and the bridge HOMO levels.

Experimental Section

The synthesis of the ligand and the metal complex has been described in detail previously.[19] Microelectrodes were prepared using platinum microwires of radii between 1 and 25 μm sealed in a glass shroud that were mechanically polished as described previously.[8] Electrochemical cleaning of the microelectrodes was carried out in 0.2 M H_2SO_4 by electrochemically cycling between limits chosen to initially oxidize and then reduce the surface of the platinum electrodes. Excessive cycling was avoided in order to minimize the extent of surface roughening. The real surface areas were determined by calculating the charge under the platinum oxide reduction peak.[20] Typical surface roughness values were between 1.6 and 2.0. Determining the real, as opposed to the geometric, area of the electrodes is important if the area of occupation of the adsorbate is to be accurately determined.

Cyclic voltammetry was performed using a CH Instruments model 660A Electrochemical Workstation and a conventional three-electrode cell. All solutions were deoxygenated thoroughly using nitrogen, and a blanket of nitrogen was maintained over the solution during all experiments. Potentials are quoted with respect to a BAS Ag/AgCl gel-filled reference electrode. All experiments were performed at room temperature (22 $\pm$ 3 °C). For short time-scale experiments (<250 μs), a custom-built function-programmable generator−potentiostat was used. This instrument had a rise time of less than 10 ns and was used to apply potential steps of variable pulse width and amplitude directly to a two-electrode cell. A large-area Pt foil and a reference electrode were combined to form a counter electrode. The foil lowered the resistance and provided a high-frequency path. The current to voltage converter was based on a Comlinear CLC 203 AI operational amplifier with a 1500-Ω feedback resistance and a response time of less than 10 ns. The chronoamperograms were recorded using a HP54201A digital oscilloscope in 64X time-average mode. Cell time constants were extracted from the slope of ln $i(t)$ vs t plots using software routines written in Microsoft Excel.

Spontaneously adsorbed monolayers were formed by immersing the microelectrode in micromolar solutions of the metal complex in methanol/water (50/50, v/v) for periods up to 12 h. The complex is stable toward aerial oxidation and no precautions were taken to exclude atmospheric oxygen during monolayer formation. Before electrochemical measurements were made, the electrodes were rinsed with acetone and electrolyte solution to remove any unbound material. Subsequent measurements were performed in blank electrolyte.

Results and Discussion

General Electrochemical Properties. Figure 1 shows representative cyclic voltammograms for a spontaneously adsorbed monolayer of $[Os(bpy)_2 4bptCl]^+$ (bpy is 2,2′-bipyridyl and 4bpt is 3,5-bis(pyridin-4-yl)-1,2,4-triazole) upon electrochemical cycling in aqueous 0.1 M $LiClO_4$ as the scan rate is systematically varied from 0.4 to 2.0 V s^{-1}. The solution does not contain any dissolved complex. The formal potential of the $Os^{2+/3+}$ redox reaction is 0.276 $\pm$ 0.005 V vs Ag/AgCl, which compares to a value of 0.249 $\pm$ 0.004 V when the complex is dissolved in acetonitrile. The fact that the solution phase formal potential of this complex is within 30 mV of that observed for the surface

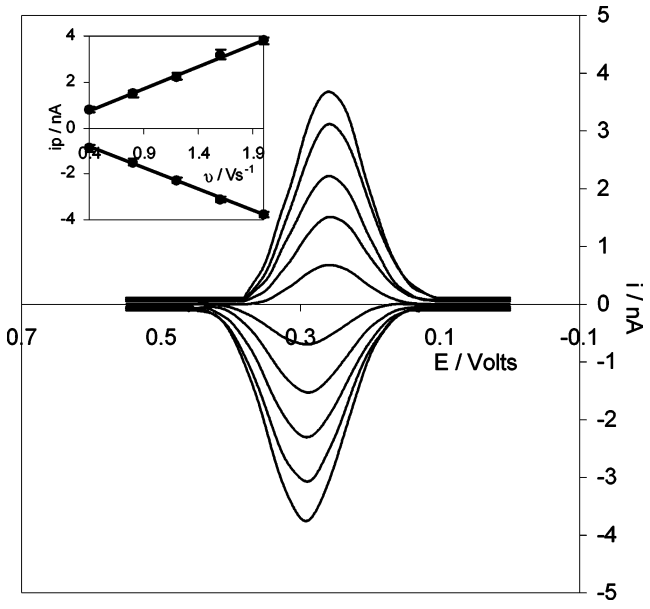

Figure 1. Cyclic voltammograms for a dense, spontaneously adsorbed monolayer of $[Os(bpy)_2 4bptCl]^+$ in 0.1 M $LiClO_4$ at an electrolyte pH of 6.0 $\pm$ 0.1. Scan rates are (from top to bottom) 2.0, 1.6, 1.2, 0.8, and 0.4 V s^{-1}. The radius of the platinum microelectrode is 25 μm. The monolayer surface coverage is 1.10×10^{-10} mol cm^{-2}. Cathodic currents are up, and anodic currents are down. Inset: Graph of i_p vs v.

confined complex suggests that these monolayers are solvated.[21] Upon repetitive cycling in this electrolyte at both high (pH 14) and low (pH 0) pH over periods up to 12 h, the peak heights change by less than 5%, indicating that these films are highly stable over a wide range of pH values.

The response obtained for these films is similar to that previously reported for structurally related complexes[22] and is consistent with that expected for an electrochemically reversible reaction involving a surface-confined species.[23] The peak shape is independent of v for $0.05 \leq v \leq 50$ V s^{-1} and, as shown in the inset of Figure 1, the peak height increases linearly with increasing scan rate, rather than the $v^{1/2}$ dependence observed for the complex dissolved in acetonitrile. Therefore, it may be concluded that $[Os(bpy)_2 4bptCl]^+$ adsorbs to the surface of the platinum electrode to give an electroactive film.

Monolayers of this complex exhibit nonzero peak−peak separations, ΔE_p, even at low scan rates; e.g., ΔE_p is 35 $\pm$ 5 mV at a scan rate of 0.5 V s^{-1}. This behavior has been reported previously for monolayers of analogous osmium polypyridyl complexes.[23,24] The ΔE_p value is independent of scan rate up to at least 50 V s^{-1}, indicating that slow heterogeneous kinetics are not responsible for the observed behavior. Ohmic effects are not responsible for this behavior as the increased currents at higher scan rates would be expected to increase the ΔE_p value. Feldberg has interpreted similar nonideal responses in terms of unusual quasireversibility (UQR), arising due to rate processes that are slow compared to the experimental time scale.[25]

Where there are no lateral interactions occurring between immobilized species and a rapid equilibrium is established with the metal electrode, the full width at half-maximum (fwhm) of either the anodic or cathodic wave is 90.6/n mV.[23] Monolayers of this complex exhibit fwhm values of 120 $\pm$ 10 mV, suggesting that there are repulsive interactions between adjacent adsorbates. The fwhm value is independent of the contacting electrolyte pH and, therefore, the charge on the bridging ligand. Thus, it appears that repulsive interactions between adjacent adsorbates are dominated by the positively charged $Os(bpy)_2Cl$ headgroups, rather than the bridging ligand.

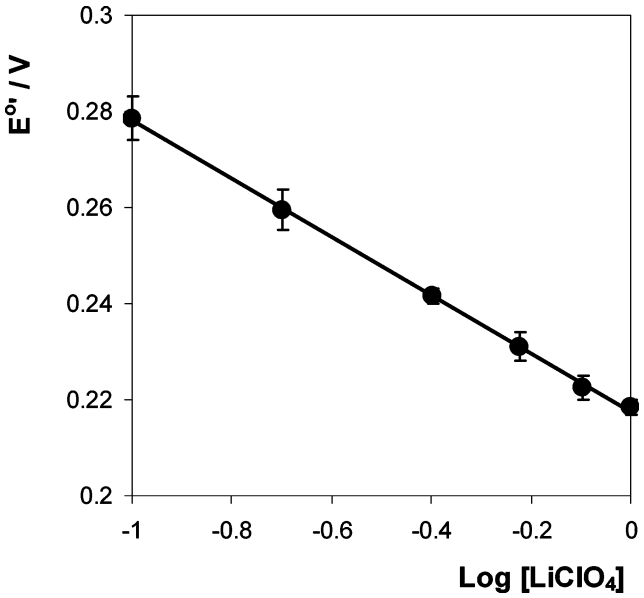

Figure 2. Effect of electrolyte concentration on the formal potential of the $Os^{2+/3+}$ process within an $[Os(bpy)_2 4bptCl]^+$ monolayer adsorbed on a 25-μm radius platinum microelectrode. All measurements were performed in a constant-background electrolyte of 1.0 M Na_2SO_4.

The surface coverage, as experimentally determined from the area under the cyclic voltammetry wave, was found to be $1.10 \pm 0.09 \times 10^{-10}$ mol cm^{-2},[23] corresponding to an area occupied per molecule of 151 ± 11 Å^2. This area is in agreement with that previously reported for this complex[19] and is comparable to that reported for similar complexes adsorbed within monolayers.[26,27]

Effects of Electrolyte Concentration and pH on Redox Energetics. Given our interest in examining redox switching dynamics and protonation reactions within these monolayers, it is important to probe the nature of the local microenvironment of the $Os^{2+/3+}$ centers. The formal potential depends on both the solvation shell and the extent of ion pairing.[28,29] By examining the effect of the electrolyte concentration on the formal potential of the redox reaction, it is possible to gain an insight into the extent of ion pairing between the immobilized redox centers and counterions from the electrolyte. The effect of electrolyte concentration on the formal potential of the $Os^{2+/3+}$ redox reaction has been examined for $0.1 \leq [LiClO_4] \leq 1.0$ M. In these measurements, scan rates less than 0.5 V s^{-1} were employed so as to avoid any influence from the interfacial charge-transfer kinetics. To avoid complications due to changes in the ionic strength of the solution, a fixed background of 1.0 M Na_2SO_4 was used as a swamping electrolyte. The formal potential of the $Os^{2+/3+}$ redox reaction shifts by less than 10 mV over the electrolyte concentration range $0.1 \leq [Na_2SO_4] \leq 1.0$ M, indicating that SO_4^{2-} has little tendency to ion pair with the osmium centers. For $0.1 \leq [LiClO_4] \leq 1.0$ M, the peak shapes and heights are independent of the electrolyte concentration. However, as illustrated in Figure 2, $E^{\circ\prime}$ shifts in a negative potential direction as the $LiClO_4$ concentration increases, indicating that it becomes increasingly easier to oxidize the osmium redox center at higher electrolyte concentrations. This behavior is consistent with ion pairing between the perchlorate and the redox center. The theoretical slope of this semilog plot is $(59/p)$ mV/decade, where p is the difference in the number of anions pairing with the oxidized and reduced forms of the redox center. The slope determined for $[Os(bpy)_2 4bptCl]^+$ monolayers was 60 ± 3 mV, indicating that a single additional anion becomes bound to the redox center in the oxidized state.

The 4bpt bridging ligand is capable of undergoing a protonation/deprotonation reaction depending on the pH of the contacting solution. Protonation of the 4bpt bridge within a monolayer will change the overall charge of the adsorbate and may affect the extent of electronic coupling between the electrode surface and the remote $[Os(bpy)_2Cl]^+$ redox center. By probing the effect of the contacting electrolyte solution on the voltammetric response of these monolayers, an insight into the effect of protonation of the 4bpt bridge may be obtained. The formal potential of the $Os^{2+/3+}$ redox reaction shifts in a positive potential direction by 40 ± 3 mV upon changing the pH of the contacting electrolyte solution from pH 12.0 to 6.0. This shift in $E^{\circ\prime}$ is fully reversible when the electrolyte pH is changed. The positive shift of $E^{\circ\prime}$ with decreasing pH indicates that oxidation of the Os^{2+} metal center becomes thermodynamically more difficult when the 4bpt bridge is protonated. Electrostatics are likely to dominate this response since protonation of the 4bpt ligand causes an increase in the overall charge on the complex. However, a reduced electron-donating ability of the ligand upon protonation may also contribute to the positive shift in $E^{\circ\prime}$. While these data clearly demonstrate that protonating the bridge influences the energetics of charge transfer, they do not provide an insight into the pK_a of the 4bpt ligand when immobilized at the electrode surface. The pK_a of the ligand may be altered upon immobilization at an electrode surface for a number of reasons. First, the dielectric constant within a dense monolayer may be distinctly different from that in bulk solution. Second, immobilization of the complex at an electrode surface may significantly alter the electron density of the ligand. Both of these effects could cause significant changes in the pK_a to be observed. Capacitance data can provide a useful insight into this issue.

Acid/Base Properties of the Triazole Bridge. Smith and White have described the limiting cases for the potential profile across a monolayer.[30] Depending on the potential distribution at the modified interface, the capacitance of the diffuse layer, C_{dif}, and the monolayer capacitance, C_{mono}, may contribute to the total interfacial capacitance, C_T, according to eq 1

$$C_T^{-1} = C_{dif}^{-1} + C_{mono}^{-1} \quad (1)$$

The capacitance of the monolayer is given by eq 2

$$C_{mono} = \epsilon_o \epsilon_{mono}/d \quad (2)$$

where ϵ_o is the permittivity of free space, ϵ_{mono} is the monolayer dielectric constant, and d is the monolayer thickness.

Potential step chronoamperometry has been used to determine the interfacial capacitance as a function of the concentration of electrolyte. This technique was chosen due to the ease of implementation and the ability to time resolve double layer charging and Faradaic currents. After a potential step, a charging current, i_c, will flow according to eq 3[31]

$$i_c(t) = \Delta E/R \exp(-t/RC_T) \quad (3)$$

where ΔE is the magnitude of the potential step, R is the cell resistance, and C_T is the total interfacial capacitance. In determination of the interfacial capacitance, 0.025 V potential steps were applied to the monolayer-modified working electrode in a potential region where no faradaic currents flow (0.400−0.425 V vs Ag/AgCl). The charging current was then measured as a function of time and linear plots of ln $i_c(t)$ vs t were used to obtain R and C_T. The potential step amplitude used in these experiments was small enough to allow the measured capaci-

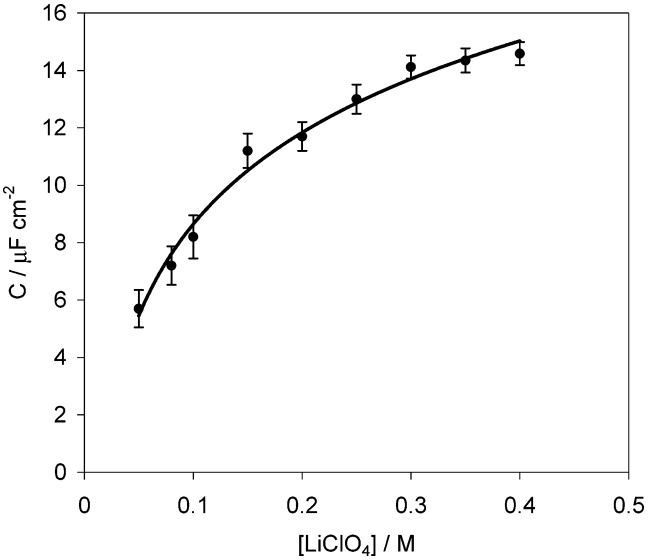

Figure 3. Dependence of the differential capacitance on $LiClO_4$ concentration for spontaneously adsorbed monolayers of $[Os(bpy)_2$4-bptCl$]^+$ on a 12.5-μm radius platinum microelectrode. The potential step size was 0.025 V and was from 0.400 to 0.425 V vs Ag/AgCl.

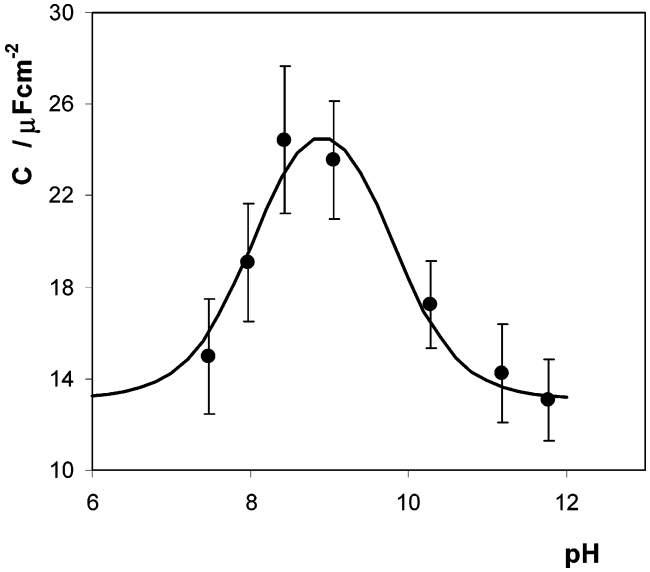

Figure 4. Effect of systematically varying the contacting electrolyte pH on the differential capacitance of monolayers of $[Os(bpy)_2$4-bptCl$]^+$ at 12.5-μm platinum microelectrode. The supporting electrolyte is aqueous 1.0 M $LiClO_4$, and the pH was altered using concentrated aqueous solutions of NaOH or $HClO_4$.

tance to be considered as an approximate differential capacitance, C_T.[19] Figure 3 illustrates the differential capacitance values determined for a 12.5-μm radius platinum microelectrode modified with a monolayer of $[Os(bpy)_2$4bptCl$]^+$ as a function of electrolyte concentration. Equation 1 indicates that the interfacial capacitance depends on the diffuse-layer capacitance and the capacitance of the monolayer. Unlike the monolayer capacitance, the diffuse-layer capacitance depends on the concentration of the electrolyte. Figure 3 clearly illustrates that the differential capacitance is sensitive to the electrolyte concentration, increasing for electrolyte concentrations up to approximately 0.3 M. At concentrations above 0.3 M, the differential capacitance is approximately 18 ± 3 μF cm^{-2} and is likely to be dominated by the monolayer capacitance. The limiting differential capacitance is significantly larger than that expected for a monolayer that is completely impermeable to electrolyte,[32] 5−10 μF cm^{-2}, suggesting that this monolayer is at least partially solvated at high electrolyte concentrations.

Figure 4 illustrates the effect of systematically varying the electrolyte pH on the differential capacitance between approximately $7.5 \leq$ pH ≤ 12.0. All changes in the differential capacitance were confirmed to be reversible by first increasing and then decreasing the pH of the contacting electrolyte solution. The shape of the curve agrees with that predicted by theory[28,30] and yields a surface pK_a of 8.9 ± 0.2. Significantly, this value is indistinguishable from that found for the complex in solution, 9.1, suggesting that immobilization does not change the acid/base properties of the bridge and that the monolayer is well solvated.

Heterogeneous Electron-Transfer Dynamics. As discussed in the Introduction, when redox switching proceeds by a superexchange mechanism, the dynamics depend on the energy difference between the redox center and bridge states. Electron transfer is expected to dominate if the redox states and the bridge LUMO are similar in energy, whereas hole transfer will be important when the $Os_{d\pi}$−HOMO separation is relatively smaller. Electron-rich π-donating linkers of the kind used here have been shown to support hole superexchange reactions.[33] Significantly, the 4bpt bridge is also capable of undergoing a protonation/deprotonation reaction depending on the pH of the contacting electrolyte solution. The measurements of the pH dependence of the formal potential presented earlier demonstrate that these acid/base reactions change the electron density on the redox center and bridge thus modulating the $Os_{d\pi}$−HOMO separation which may change the rate constant for heterogeneous electron transfer.

To determine the rates of heterogeneous electron transfer across the electrode/monolayer using this system, high-speed chronoamperometry has been employed. Chronoamperometry has three distinct advantages over cyclic voltammetric experiments for extracting kinetic data.[9] First, the kinetics for different potentials (i.e., different reaction free energies) are not convoluted by a potential scan. Second, the kinetic homogeneity of the sites can be judged by the functional form of the current transient. Third, electron-transfer rates can be measured far from $E^{\circ\prime}$, i.e., at large reaction free energies. Once double-layer charging is complete, for an ideal electrochemical reaction involving a surface confined species, the Faradaic current, i_F, following a potential step that changes the redox composition of the monolayer exhibits a single-exponential decay in time according to[6,13]

$$i_F(t) = kQ \exp(-kt) \tag{4}$$

where k is the apparent rate constant for the reaction and Q is the total charge passed in the redox transformation. Figure 5 illustrates typical chronoamperometric responses for the oxidation of a monolayer of $[Os(bpy)_2$4bptCl$]^+$ on a 2.5-μm radius platinum microelectrode where the electrolyte is aqueous 1.0 M $LiClO_4$, adjusted to pH 12. In these experiments, the overpotential ($E - E^{\circ\prime}$) was 0.148 and −0.181 V (solid line and broken line, respectively). A 500-mV potential step was employed in these experiments from a potential where no Faradaic reaction occurred at the electrode/monolayer interface to a potential where the Faradaic reaction of interest (oxidation or reduction) occurred. As Figure 5 represents the current responses for both an oxidation ($\eta = 0.148$ V) and a reduction reaction ($\eta = -0.181$ V), we have illustrated the absolute current response as a function of time. This figure shows that on a submicrosecond time scale, two current decays can be separated. These responses, which arise from double-layer charging and

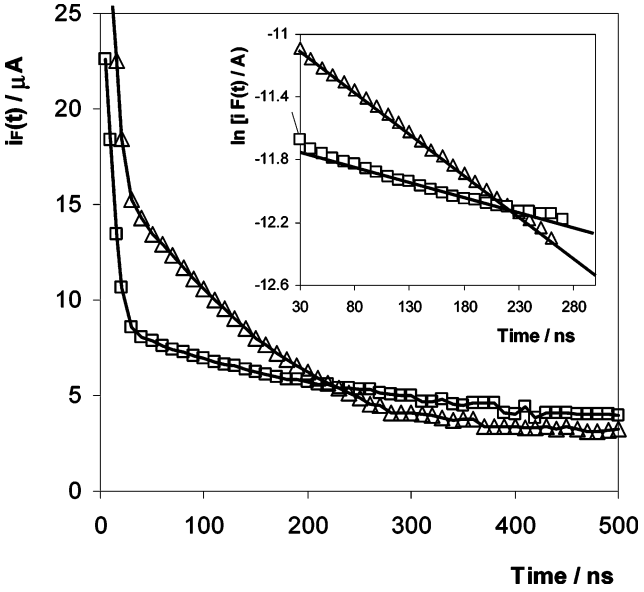

Figure 5. Absolute current response for a 2.5-μm radius platinum microelectrode modified with a monolayer of [Os(bpy)$_2$4bptCl] following a potential step where the overpotential is 0.148 V (△) and −0.181 V (□). The supporting electrolyte is aqueous 1.0 M $LiClO_4$ adjusted to pH 12.0 with NaOH. Inset: ln $i_F(t)$ vs t.

Faradaic current flow, are time resolved due to the much shorter time constant of double-layer charging compared to that of the Faradaic reaction.

By measuring the current response far from $E^{\circ\prime}$ or by analyzing only the initial part of the decay in transients such as those illustrated in Figure 5, the *RC* time constant of the 2.5-μm microelectrode has been determined 15 ± 4 ns. This rapid response to changes in the applied potential allows semilog plots of ln $i_F(t)$ vs t, such as those illustrated in the inset of Figure 5, to be used to extract kinetic information from this system. Faradaic currents were recorded only at times that were 5−10 times that of the *RC* constant. At these times, the contribution of the charging current to the overall current is negligible. The linearity of the ln $i_F(t)$ vs t plots shown in the inset of Figure 5 indicates that electron transfer is characterized by a single rate constant over the time required to collect greater than 95% of the total charge for the redox reaction. Deviations from linearity would be expected if ohmic drop were present. Uncompensated resistance would cause the potential, and hence the apparent rate, to evolve with time. Therefore, *iR* drop would cause deviations to be observed at short experimental times. All of the transients recorded displayed nearly ideal chronoamperometric responses, suggesting that ohmic losses are negligible. The apparent rate constants for the oxidation and reduction of the Os^{2+} redox centers, obtained from the semilog plot shown in Figure 5 in conjunction with eq 4, are 5.3×10^6 and 3.4×10^6 s^{-1} for overpotentials of 148 and −181 mV, respectively. Given that the *RC* time constant of the platinum microelectrode is approximately 15 ns, the maximum rate constant that can be determined is approximately 10^7 s^{-1}. A Tafel plot of ln k vs overpotential for a monolayer of [Os(bpy)$_2$4bptCl]$^+$ in which the supporting electrolyte is 1.0 M $LiClO_4$ adjusted to pH 12.5 with NaOH is illustrated in Figure 6. For overpotentials less than about 250 mV, ln k depends approximately linearly on the overpotential, which is consistent with the Butler−Volmer formulation of the potential dependence of electrochemical reaction rates. Moreover, the fact that linear responses are observed for both the oxidation and reduction of the monolayers of overpotentials up to 250 mV suggests that the Marcus reorganization energy[19] is at least 30 kJ mol^{-1}.

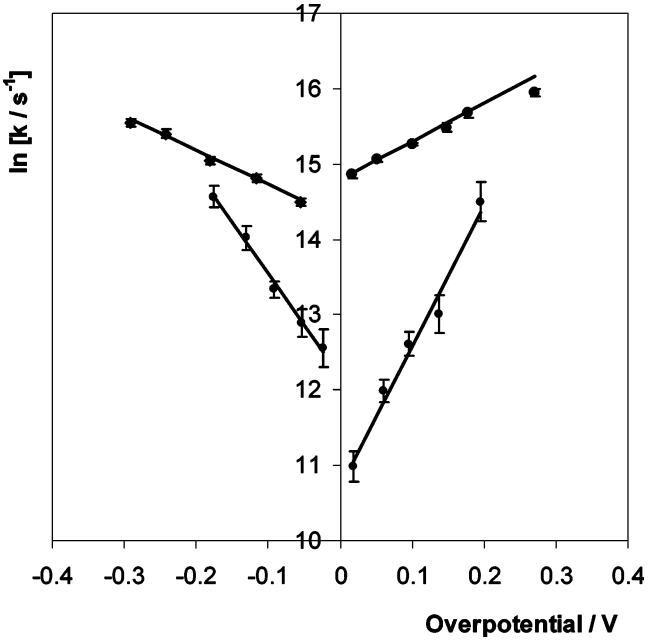

Figure 6. The upper lines illustrate a Tafel plot of ln k vs overpotential for a 2.5-μm radius platinum microelectrode modified with a monolayer of [Os(bpy)$_2$4bptCl]. The supporting electrolyte is aqueous 1.0 M $LiClO_4$ adjusted to pH 12.5 with concentrated NaOH. The lower lines illustrate a Tafel plot where the supporting electrolyte is aqueous 1.0 M $LiClO_4$ at a of pH 5.5. Where error bars are not visible, errors are approximately equal to the size of the symbols.

As illustrated in Figure 6, specifying the overpotential with respect to the formal potential determined using cyclic voltammetry gives rate constants that are not equal for zero overpotential. Figure 6 illustrates that for $\eta = 0$, "standard" heterogeneous electron-transfer rate constants of 1.60×10^6 and 2.7×10^6 s^{-1} for reduction and oxidation of the monolayer are obtained, respectively. The nonequal intercepts at $\eta = 0$ in Figure 6 suggest that the effective formal potential in short time scale chronoamperometry (i.e., the potential where the forward and backward reaction rate are equal) is shifted by approximately −40 mV compared to the cyclic voltammetry value. This may be due to the influence of ion pairing. Because of the relatively long time scale involved, the cyclic voltammetry $E^{\circ\prime}$ represents a fully ion-paired situation, whereas high-speed chronoamperometry may not allow sufficient time for the Os^{3+} site to become ion-paired with an extra perchlorate anion. Figure 6 also illustrates a Tafel plot for an adsorbed [Os(bpy)$_2$4bptCl] monolayer where the supporting electrolyte is 1.0 M $LiClO_4$ at a pH of 5.5. This graph also shows a shift of the apparent chronoamperometric $E^{\circ\prime}$ value compared to the cyclic voltammetry $E^{\circ\prime}$. However, in contrast to the high pH data, at low pH the apparent $E^{\circ\prime}$ shifts in a positive potential direction. This result is consistent with the protonated and deprotonated monolayers undergoing different extents of ion pairing perhaps at different rates. The "standard" heterogeneous electron-transfer rate constants determined at $\eta = 0$ (based on the cyclic voltammetry formal potential) are 1.9×10^5 and 4.5×10^4 s^{-1} for the reduction and oxidation processes, respectively, which agrees with previously reported data obtained for protonated monolayers.[19]

The most significant conclusion of these data is that the redox switching rate for monolayer reduction decreases by approximately an order of magnitude upon protonation of the 4bpt ligand. The switching rate for the oxidation reaction decreases by a larger amount, almost 2 orders of magnitude, upon protonation of the 4bpt bridging ligand. As illustrated in Figure

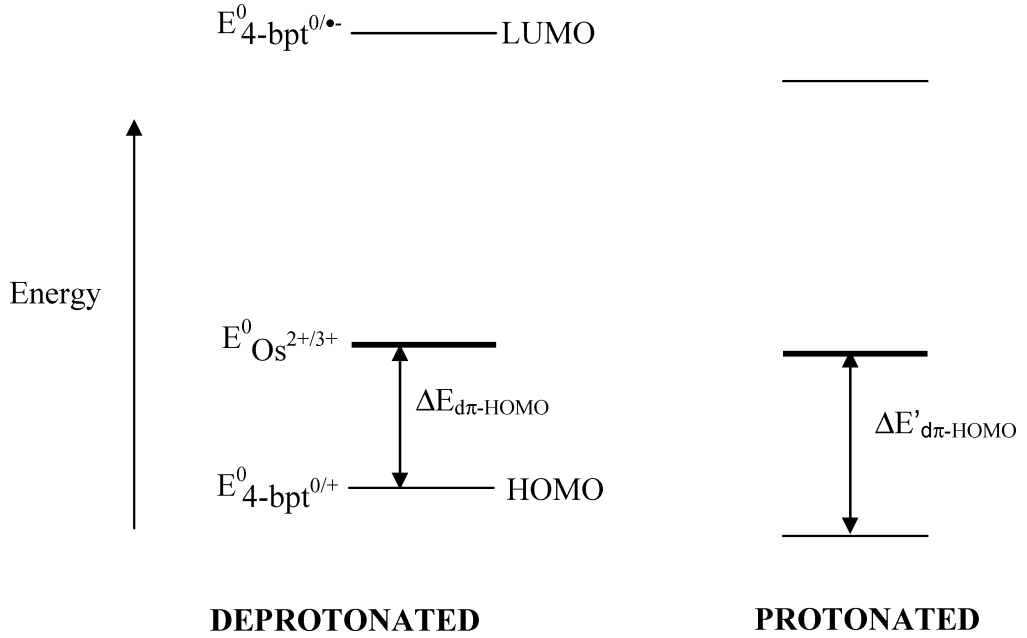

Figure 7. Proposed effect of protonation of the 4bpt bridging ligand on hole superexchange.

7, protonation of the 4bpt bridging ligand will decrease the electron density on the ligand, making it harder to oxidize and easier to reduce the bridge. This will cause the formal potential of the HOMO and the LUMO of the bridge to shift in a positive potential direction, thereby increasing the $Os_{d\pi}$−HOMO separation, causing slower redox switching dynamics to be observed for the protonated monolayer. These data also provide an insight into the mechanism of charge transfer, i.e., hole vs electron transfer. If the dominant superexchange mechanism was electron superexchange, the decreased $Os_{d\pi}$−LUMO separation should cause an increase in the rate of electron transfer upon protonation of the bridging ligand. The decrease observed in switching dynamics upon protonation suggests that redox-switching transfer occurs via a hole-transfer superexchange mechanism.

Conclusions

Stable close-packed monolayers of $[Os(bpy)_2 4bptCl]PF_6$ have been formed on platinum microelectrodes. The adsorbed monolayers exhibit well-defined voltammetric responses for $1.0 < pH < 12.0$. Probing the pH dependence of the interfacial capacitance reveals that the triazole bridging ligand is capable of undergoing a protonation/deprotonation reaction with a pK_a of 8.9 ± 0.6. This value is indistinguishable from that found for the complex in solution, suggesting that the adsorbates are well solvated within the monolayer.

High-speed chronoamperometry has been used to probe the rate of heterogeneous electron transfer across the electrode/monolayer interface. Significantly, upon protonation of the 4-bpt bridge, the standard heterogeneous charge-transfer rate constant decreases by more than 1 order of magnitude for both the oxidation and reduction reactions. This observation is consistent with mediating electronic states within the bridging ligand (superexchange) playing an important role in the redox switching process. Specifically, the results suggest that hole transfer is mediated through the HOMO of the 4-bpt ligand. Protonating the bridge reduces its electron density thus lowering the energy of the bridge HOMO relative to the hole acceptor states of the osmium and decreasing the standard rate constant.

Acknowledgment. The financial support of Enterprise Ireland, the Irish Science and Technology Agency, the Higher Education Authority under the Program for Research in Third Level Institutions, and the generous loan of potassium hexachloro osmate by Johnson−Matthey are gratefully acknowledged.

References and Notes

(1) Kropf, M.; van Loyen, D.; Schwarz, O.; Durr, H. *J. Phys. Chem. A* **1998**, *102*, 5499.
(2) Moser, C. C.; Keske, J. M.; Warnacke, K.; Farid, R. S.; Dutton, P. L. *Nature* **1992**, *355*, 796.
(3) Gust, D.; Moore, T. A.; *Science* **1989**, *244*, 35.
(4) *Molecular Design of Electrode Surfaces*; Murray, R. W., Ed.; Wiley: New York, 1992; Vol. 22.
(5) Chidsey, C. E. D.; Murray, R. W. *Science* **1986**, *231*, 25.
(6) Finklea, H. O.; Hanshaw, D. D. *J. Am. Chem. Soc.* **1992**, *114*, 3173.
(7) Finklea, H. O.; Liu, L.; Ravenscroft, M. S.; Punturi, S. *J. Phys. Chem.* **1996**, *100*, 18852.
(8) Forster, R. J.; Faulkner, L. R. *J. Am. Chem. Soc.* **1994**, *114*, 5444.
(9) Chidsey, C. E. D. *Science* **1991**, *251*, 919.
(10) Finklea, H. O.; Ravenscroft, M. S.; Snider, D. A. *Langmuir* **1993**, *9*, 223.
(11) Ravenscroft, M. S.; Finklea, H. O. *J. Phys. Chem.* **1994**, *98*, 3843.
(12) Ju, H.; Leech, D.; *Phys. Chem. Chem. Phys.* **1999**, *1*, 1549.
(13) Forster, R. J.; Faulkner, L. R. *J. Am. Chem. Soc.* **1994**, *116*, 5453.
(14) Cheng, J.; Sághi-Szabó, G.; Tossell, J., A.; Miller, C. J. *J. Am. Chem. Soc.* **1996**, *118*, 680.
(15) Sumner, J. J.; Weber, K. S.; Hockett, L. A.; Creager, S. E. *J. Phys. Chem. B* **2000**, *104*, 7449.
(16) Sumner, J. J.; Creager, S. E. *J. Am. Chem. Soc.* **2000**, *122*, 11914.
(17) Sek, S.; Bilewicz, R.; *J. Electroanal. Chem.* **2001**, *509*, 11.
(18) McConnell, H. M. *J. Chem. Phys.* **1961**, *35*, 508.
(19) Forster, R. J.; Keyes, T. E.; Vos, J. G. *Analyst* **1998**, *123*, 1905.
(20) Trasatti, S.; Petrii, O. A. *J. Electroanal. Chem.* **1992**, *327*, 354.
(21) Forster, R. J. O'Kelly, J. P. *J. Phys. Chem.* **1996**, *100*, 3695.
(22) Forster, R. J.; Figgemeier, E.; Loughman, P.; Lees, A.; Hjelm, J.; Vos, J. G. *Langmuir* **2000**, *16*, 7871.
(23) Bard, A. J.; Faulkner, L. R. *Electrochemical Methods: Fundamentals and Applications*, 2nd ed.; Wiley: New York, 2001.
(24) Forster, R. J.; Faulkner, L. R. *Langmuir* **1995**, *11*, 1014.
(25) Feldberg, S. W.; Rubinstein, I. *J. Electroanal. Chem.* **1988**, *240*, 1.
(26) Tirado, J. D.; Abruña, H. D. *J. Phys. Chem.* **1996**, *100*, 4556.
(27) Hudson, J. E.; Abruña, H. D. *J. Phys. Chem.* **1996**, *100*, 1036.
(28) Rowe, G. K.; Creager, S. E. *Langmuir* **1991**, *7*, 2307.
(29) Creager, S. E.; Rowe, G. K. *Anal. Chim. Acta* **1991**, *246*, 233.
(30) Smith, C. P.; White, H. S. *Anal. Chem.* **1992**, *64*, 2398.
(31) Wightman, R. M.; Wipf, D. O.; In *Electroanalytical Chemistry*; Bard, A. J., Ed.; Marcel Dekker: New York, 1989; Vol. 15.
(32) Porter, M. D.; Bright, T. B.; Allara, D. L.; Chidsey, C. E. D. *J. Am. Chem. Soc.* **1987**, *109*, 3559.
(33) Barigelletti, F.; De Cola, L.; Balzani, V.; Hage, R.; Haasnoot, J. G.; Reedijk, J.; Vos, J. G. *Inorg. Chem.* **1989**, *28*, 4344.